Epithelial Splicing Regulatory Protein 1 (ESRP1) is a new regulator of stomach smooth muscle development and plasticity

Sébastien Sagnol, Stéphane Marchal, Yinshan Yang, Frédéric Allemand, Pascal de Santa Barbara

Developmental Biology 414 (2016) 207–218

Epithelial Splicing Regulatory Protein 1 (ESRP1) is a new regulator of stomach smooth muscle development and plasticity

Sébastien Sagnol [a], Stéphane Marchal [a], Yinshan Yang [b], Frédéric Allemand [b], Pascal de Santa Barbara [a,*]

[a] PhyMedExp, INSERM U1046, CNRS UMR 9214, University of Montpellier, 34295 Montpellier cedex 5, France
[b] Centre de Biochimie Structurale, CNRS UMR 5048, INSERM U1054, University of Montpellier, 34295 Montpellier cedex 5, France

A B S T R A C T

In vertebrates, stomach smooth muscle development is a complex process that involves the tight transcriptional or post-transcriptional regulation of different signalling pathways. Here, we identified the RNA-binding protein Epithelial Splicing Regulatory Protein 1 (ESRP1) as an early marker of developing and undifferentiated stomach mesenchyme. Using a gain-of-function approach, we found that in chicken embryos, sustained expression of *ESRP1* impairs stomach smooth muscle cell (SMC) differentiation and *FGFR2* splicing profile. ESRP1 overexpression in primary differentiated stomach SMCs induced their dedifferentiation, promoted specific-*FGFR2b* splicing and decreased FGFR2c-dependent activity. Moreover, co-expression of ESRP1 and RBPMS2, another RNA-binding protein that regulates SMC plasticity and Bone Morphogenetic Protein (BMP) pathway inhibition, synergistically promoted SMC dedifferentiation. Finally, we also demonstrated that ESRP1 interacts with RBPMS2 and that RBPMS2-mediated SMC dedifferentiation requires ESRP1. Altogether, these results show that ESRP1 is expressed also in undifferentiated stomach mesenchyme and demonstrate its role in SMC development and plasticity.

Keywords:
Gastrointestinal tract
Smooth muscle
Chick
RNA-binding protein
FGF pathway
ESRP1

1. Introduction

The vertebrate gastrointestinal (GI) tract develops from a simple and uniform tube into a complex organ with specific differentiation patterns along the anterior–posterior axis (Faure and de Santa Barbara, 2011). The gastrointestinal mesenchyme originates from the splanchnopleural mesoderm and differentiates along the radial axis, giving rise to the smooth muscle and submucosal layers (de Santa Barbara et al., 2002). Early during development, the Hedgehog morphogen sends signals from the GI epithelium to the adjacent mesenchyme to control its growth and differentiation by regulating several signalling pathways, such as the Bone Morphogenetic Protein (BMP), Fibroblast Growth Factor (FGF) and NOTCH pathways (de Santa Barbara et al., 2005; Notarnicola et al., 2012; Le Guen et al., 2009; Faure et al., 2015). The differentiation of gastrointestinal mesenchymal cells into smooth muscle cells (SMCs) is characterized first by their elongation and clustering. This is followed by SMC determination, which is mainly associated with the early expression of alpha smooth muscle actin (αSMA), and then SMC differentiation, which is characterized by the expression of proteins involved in smooth muscle contractility, such as CALPONIN (Gabella, 2002; Le Guen et al., 2015).

In contrast to skeletal muscle, paediatric and adult SMCs do not terminally differentiate and maintain a remarkable capacity to dedifferentiate and proliferate (defined as SMC plasticity). Indeed, following exogenous/endogenous stimuli or injury, all SMCs, independently of their embryonic origin (vascular or visceral), have the unique ability to switch from a differentiated, quiescent contractile state to an undifferentiated and highly proliferative state (Le Guen et al., 2015; Scirocco et al., 2016). Reactivation of developmental processes in differentiated SMCs, through upregulation of the BMP and/or FGF signalling pathways, induces their dedifferentiation (Notarnicola et al., 2012; Le Guen et al., 2009).

Proper regulation of smooth muscle development and plasticity entails the tight and long-term control of several signalling pathways, usually at the post-transcriptional level. This is generally performed at multiples steps of RNA metabolism, such as RNA transport and sub-cellular localization, splicing, translation and degradation. These mechanisms involve specific regulatory proteins, such as RNA-binding proteins. The human genome includes about 500 genes encoding RNA-binding proteins, each interacting with different affinities and specificities with RNAs. RNA-binding proteins are key regulators of RNA metabolism by controlling the temporal, spatial and functional dynamics of RNAs (Kwon et al., 2013; Gerstberger et al., 2014). Using a microarray approach to find candidate genes involved in stomach mesenchyme

* Corresponding author.
E-mail address: Pascal.de-Santa-Barbara@inserm.fr (P. de Santa Barbara).

development (Le Guen et al., 2009), we identified *RBPMS2*, a gene that encodes an RNA-binding protein (Notarnicola et al., 2012). We found that in chicken embryos, RNA-Binding Protein with Multiple Splicing-2 (RBPMS2) is strongly expressed during the early stage of gastrointestinal mesenchyme precursor development and is quickly down-regulated in differentiated and mature SMCs (Notarnicola et al., 2012). RBPMS2 positively regulates *NOGGIN* mRNA expression, a major inhibitor of the BMP pathway, through the formation of a *NOGGIN*-RBPMS2 ribonucleoprotein complex, and inhibits the BMP pathway activity (Notarnicola et al., 2012; Sagnol et al., 2014). Misexpression of RBPMS2 in differentiated gastrointestinal SMCs induces their dedifferentiation (Notarnicola et al., 2012; Sagnol et al., 2014). Moreover, RBPMS2 homodimerization, through a specific motif located in its unique RRM domain, is required to lead RBPMS2-dependent SMC dedifferentiation (Sagnol et al., 2014).

Epithelial Splicing Regulatory *(ESRP1)* is another gene encoding an RNA-binding protein discovered using the microarray approach that identified RBPMS2 (Le Guen et al., 2009; Notarnicola et al., 2012). ESRP1 was previously detected exclusively in GI epithelia of adult mice (Warzecha et al., 2009a; Bebee et al., 2015) and in the developing intestinal epithelium (Revil and Jerome-Majewska, 2013). ESRP1 was initially identified as a regulator of *FGFR2* splicing (Warzecha et al., 2009a, 2009b), but then it was shown to regulate the splicing of many other mRNAs, such as *CD44* and *CTNND1* (Warzecha et al., 2010; Bebee et al., 2015). Moreover, ESRP1 prevents epithelial to mesenchymal transition (Brown et al., 2011) and plays multiple roles in tumour progression (Yae et al., 2012; Brown et al., 2011).

In this study, we show that the RNA-binding protein ESRP1 is expressed in the developing and undifferentiated stomach mesenchyme of chicken embryos. We found that sustained *ESRP1* expression impairs SMC differentiation *in vivo* and stimulates dedifferentiation of primary SMC cultures. These effects are associated with a change in *FGFR2* splicing. Finally, we demonstrated that ESRP1 interacts with RBPMS2 and that the RBPMS2-dependent control of SMC plasticity requires ESRP1. Together, these data provide support for an unexpected function of ESRP1 in regulating SMC development and plasticity.

2. Materials and methods

2.1. Constructs and cell lines

Chick full-length *ESRP1* cDNAs were isolated and subcloned in the pGEM-T Easy plasmid (Promega). *ESRP1*, *ESRP1* 5′Δ^{XhoI}, *ESRP1* 5′Δ, *ESRP1* 3′Δ were subcloned in the pCS2 vector with an in frame N-terminal HA-tag and the CMV promoter. The cDNA sequence that includes the third RRM domain of human ESRP1 (amino acids 439–539) was subcloned in pET22b (pET22b-*ESRP1*-RRM3). The shRNA against *Gallus gallus ESPR1* (target sequence: AGATGGAGCTTGTGGACGA) subcloned in the psi-GFP-U6 vector was from GeneCopoeia (CD-SH144J-CU6, Labomics, Belgium). Chick *ESRP1* cDNA was cloned in the RCAS vector to produce the RCAS-*ESRP1* plasmid. Myc-tagged chick full-length *RBPMS2* (RCAS-Myc-*RBPMS2*), *GFP* (RCAS-*GFP*) and Myc-*NICD* were previously described (Notarnicola et al., 2012; Le Guen et al., 2009; Faure et al., 2015). Myc-tagged chick full-length *RBPMS2* with the L40E mutation (RCAS-Myc-*RBPMS2*-L40E) was previously described and characterized (Sagnol et al., 2014). All plasmids were checked by DNA sequencing and for protein expression. Expression plasmids were transfected in DF-1 cells (a chicken fibroblast cell line from ATCC-LGC), as previously described (Moniot et al., 2004; Sagnol et al., 2014).

2.2. Avian retroviral misexpression system and analysis

Fertilized White Leghorn eggs from Haas Farm (France) were incubated at 38 °C in humidified incubators. *ESRP1* retroviral constructs were transfected in DF-1 cells to produce retroviruses that were injected in the splanchnopleural mesoderm of stage 10 chicken embryos to target the stomach mesenchyme (Moniot et al., 2004; Sagnol et al., 2014). Eggs were then placed at 38 °C until harvest. Dissected GI tissues (Moniot et al., 2004) were fixed in 4% paraformaldehyde at room temperature (RT) for 30 min, washed in PBS, gradually dehydrated in methanol and stored at −20 °C before processing for whole-mount *in situ* hybridization, as previously described (Faure et al., 2013). For tissue sections, GI tissues were fixed in 4% paraformaldehyde at RT for 30 min, washed in PBS, gradually dehydrated in ethanol and embedded in paraffin. 10-μm sections were cut using a microtome and collected on poly-L-lysine-coated slides (Thermo Fisher) for immunofluorescence or *in situ* hybridization (Faure et al., 2013). Partial chick *ESRP1* cDNA was isolated by RT-PCR from total mRNA extracts of embryonic day 5 (E5) stomachs, subcloned and sequenced. The antisense *ESRP1* RNA probe was generated using the chick *ESRP1* template by reverse transcription with incorporation of digoxigenin-labelled UTP (Roche). *BAPX1*, *FGFR2b* and *FGFR2c* antisense riboprobes were described previously (Faure et al., 2013; Nishita et al., 2011). Anti-digoxigenin antibodies coupled to alkaline phosphatase (Roche) were used to detect *ESRP1* or *BAPX1* mRNA/antisense complexes with the BM Purple solution (Roche). Images from *in situ* hybridization were acquired using a Nikon-AZ100 stereomicroscope. Immunofluorescence studies were performed on paraffin sections using rabbit anti-αSMA (Sigma-Aldrich, 1:400 dilution), mouse anti-CALPONIN (Sigma, 1:400 dilution), mouse anti-TUJ1 (Covance, 1:800 dilution), and anti-CALDESMON (1:400 dilution) (Hnia et al., 2008) antibodies. Nuclei were stained with Hoechst (Molecular Probes). Images were acquired using a Carl-Zeiss Axio Imager microscope.

2.3. Primary SMC cultures and analyses

Primary SMC cultures from E15 gizzard muscle were prepared as described (Notarnicola et al., 2012; Sagnol et al., 2014). Briefly, the *tunica muscularis* was carefully separated from the *serosa* and *tunica mucosa* before cell dissociation in 0.25 mg/mL collagenase-IA and 0.25 mg/mL soybean trypsin inhibitor (Sigma-Aldrich). To maintain SMC differentiation (more than 95% of isolated cells were DESMIN- and αSMA-positive), isolated cells were cultured for 18 h in DMEM with 20 mM HEPES, 100 U/mL penicillin, 100 μg/mL streptomycin, 2.5 μg/mL amphotericin B, 0.2% BSA and 5 μg/mL insulin on collagen I-coated plates or fibronectin-coated coverslips. Differentiated SMCs were then directly infected or resuspended in Accutase™ solution (Sigma-Aldrich) before electroporation of different expression constructs using the Neon Transfection System (Life Technologies), according to the manufacturer's instructions. For immunodetection, rabbit anti-Myc (Sigma-Aldrich, 1:200 dilution), mouse anti-HA (InvivoGen, 1:200), mouse anti-CALPONIN (Sigma-Aldrich, 1:400 dilution), and rabbit anti-αSMA (Sigma-Aldrich, 1:400 dilution) antibodies were used. When two antibodies from the same species had to be used for analysis, an unconjugated Fab fragment of goat anti-rabbit or anti-mouse IgG (H+L) (Jackson Immuno-Research, 1:20 dilutions) was used to cover the first antibody in order to present it as different species, according to the Jackson Immuno-Research's recommendations. Secondary anti-mouse, anti-rabbit or anti-goat IgG coupled to Alexa-488, -555 or -647 (Life Technologies) were used. Nuclei were stained with Hoechst (Molecular Probes). Images were acquired using a Carl-Zeiss Axio Imager microscope.

2.4. FGF9/FGFR2 pathway analysis

Primary SMCs were plated and 24 h after they were infected with empty-, *GFP*-, *ESRP1*- or *RBPMS2*-expressing retroviruses for six days. Prior to incubation with recombinant FGF9, cells were treated with 30 μM SU5402 (inhibitor of the FGF pathway) (Calbiochem) in DMEM with 20 mM HEPES, 0.2% BSA and 5 μg/mL insulin at 37 °C for 2 h, except in control cells (no SU5402/no FGF9). SU5402-treated cells were then rinsed twice with PBS and incubated in DMEM with 20 mM HEPES, 0.2% BSA and 5 μg/mL insulin, supplemented with 10 μg/mL heparin (Sigma-Aldrich) and 10 ng/mL recombinant human FGF9 (Peprotech), at 37 °C for 15 min. FGF9 induction was stopped by transferring the plates on ice and by rinsing twice with cold PBS/2 mM activated sodium orthovanadate. Cells were scraped in cold PBS/2 mM activated sodium orthovanadate and proteins were then extracted and analysed by western blotting.

2.5. Cell sorting

Primary SMCs were grown for 18 h and then electroporated with different plasmids to express GFP-tagged proteins using the Neon Transfection System (Life Technologies). 24 h after electroporation, cells were harvested by incubation with Accutase™ (Sigma-Aldrich) at 37 °C for 10 min. SMCs were then filtered through a 40 μm mesh and centrifuged at 300*g* for 5 min. SMCs were resuspended in PBS/4% BSA in FACS tubes and then analysed and sorted using a BD Biosciences FACS Aria sorter (488-nm excitation laser; 525-nm emission filter) at the Montpellier RIO Imaging facility. After assessing the forward (FSC) and side scatter (SSC), a first GFP-positive gate was set relative to the basal fluorescence levels obtained from a GFP-negative SMC sample. A second refined gate was then obtained using FSC-Area over FSC-Width to eliminate cell doublets. GFP-positive cells were then sorted and collected in cold PBS/4% BSA. Proteins were extracted from sorted cells and analysed by western blotting.

2.6. Protein extraction and western blotting

Cells were lysed by multiple freezing/thawing cycles in lysis buffer (20 mM Tris pH8, 50 mM NaCl, 1% NP40, cOmplete™ EDTA-free Protease Inhibitor Cocktail (Roche), 2 mM activated orthovanadate (Sigma-Aldrich) and PhosStop (Roche)). Protein concentration was determined using the RC DC™ Protein Assay kit (BioRad). Diluted protein samples were boiled in SDS-PAGE buffer, separated by SDS-PAGE in 12% acrylamide/BisAcrylamide gels and transferred to nitrocellulose membranes at 100 V for 1 h. Membranes were incubated according to the Odyssey technology protocol (LI-COR Biosystems) with the following primary antibodies: rabbit anti-phosphorylated p42/44 MAP kinase (phosphorylated ERK1/2, Cell Signalling, 1:2000 dilution), rabbit anti-p42/44 MAP kinase (ERK1/2, Cell Signalling, 1:1000 dilution), rabbit anti-phosphorylated AKT (Cell Signalling, 1:1000 dilution), rabbit anti-AKT (Cell Signalling, 1:1000 dilution), rabbit anti-ESRP1 (Aviva Bio System, ARP42489, 1:200 dilution), mouse anti-CALPONIN (Sigma-Aldrich, 1:5000 dilution), mouse anti-αSMA (AbCam, 1:5000 dilution), mouse anti-VINCULIN (Developmental Studies Hybridoma Bank, 1:500 dilution), rabbit anti-GFP (Torrey Pines Biolabs Inc, 1:10,000 dilution), mouse anti-HA (InvivoGen, 1:500 dilution), rabbit anti-Myc (Sigma-Aldrich, 1:1000 dilution), rabbit anti-HA (Thermo Scientific, 1:2000 dilution), rabbit anti-HISTONE H1.4 (Sigma-Aldrich, 1:4000 dilution) and rabbit anti-GAPDH (Sigma-Aldrich, 1:2000 dilution). Immunoblots were quantified using infrared-labelled secondary antibodies and the Odyssey infrared imaging system (LI-COR Biosystems).

2.7. In situ Proximity Ligation Assay (PLA)

For DuoLink *in situ* PLA (Soderberg et al., 2008; Sagnol et al., 2014), DF-1 cells were transfected using Lipofectamin-2000 (Life Technologies) and different plasmid combinations and then incubated with mouse anti-HA (Santa Cruz Biotechnologies) and rabbit anti-Myc (Sigma-Aldrich) antibodies, followed by nucleotide-conjugated secondary antibodies (rabbit PLA probe MINUS and mouse PLA probe PLUS; OLINK Biosciences, Uppsala Sweden) in saturation solution (PBS, 0.1% Tween, 5% normal donkey serum). Secondary anti-mouse and anti-rabbit IgG coupled to Alexa488 and Alexa555 (Life Technologies) were also used to detect protein expression. The Minus and Plus PLA probes interact with a rolling-circle nucleotide template when the distance between them is smaller than 40 nm. These complexes were ligated in the presence of a ligase in hybridization solution. The circular template was then amplified using a polymerase, while far-red-labelled probes hybridized with the amplified sequence, according to the manufacturer's instructions. *In situ* PLA images were acquired using a Carl-Zeiss LSM780 confocal microscope at the Montpellier RIO Imaging facility or a Carl-Zeiss Axio Imager microscope.

2.8. Immunoprecipitations

DF-1 cells were lysed in lysis buffer (20 mM Tris pH8, 50 mM NaCl, 1% NP40, cOmplete™ EDTA-free Protease Inhibitor Cocktail (Roche)). 50 μg of total protein lysates were incubated in immunoprecipitation buffer (50 mM Tris pH8, 150 mM NaCl, 0.4% NP40, cOmplete™ EDTA-free Protease Inhibitor Cocktail (Roche)) with rabbit anti-Myc antibodies (Ozyme) pre-adsorbed to protein A-Sepharose CL-4B (GE Healthcare) at 4 °C for 1 h. After extensive washing, protein samples were analysed by western blotting.

2.9. NMR spectroscopy and structure calculations

For $^{13}C/^{15}N$ isotopic labelling, human ESRP1-RRM3 was produced in *Escherichia coli* BL21λDE3 cells in M9 medium containing ^{13}C-glucose and ^{15}N-NH4Cl, and then purified and concentrated, as previously described (Sagnol et al., 2014). Nuclear Magnetic Resonance (NMR) spectroscopy was performed with 0.6 mM $^{15}N/^{13}C$-labelled recombinant ESRP1-RRM3 dissolved in 20 mM Na_2HPO_4/KH_2PO_4 buffer, 150 mM NaCl, pH 5.4 with 5% D_2O as an internal lock, as previously described (Sagnol et al., 2014). The chemical shifts were deposited in the BioMagResBank under the accession number BMRB-11601. The rms deviations were calculated with MOLMOL (Supplemental Table 1). Fifteen selected structure coordinates were deposited in the Protein Data Bank (PDB) under the accession number 2RVJ.

2.10. Reverse transcription and quantitative polymerase chain reaction (RT-qPCR)

Total RNA was extracted from stomachs or cultured cells with the HighPure RNA Isolation Kit (Roche). For stomach mesenchymal and epithelial cell dissociation, whole stage 24 (E4.5) stomachs were harvested in PBS solution. After collagenase treatment (Sigma-Aldrich) at RT for 12 min, the mesenchymal layer was isolated using fine forceps (Simon-Assmann and Kedinger, 2000; Le Guen et al., 2009). Reverse transcription was performed with the Verso cDNA Synthesis Kit (Thermo Scientific) and qPCR using the LightCycler technology (Roche Diagnostics). PCR primers (Supplemental Table 2) were designed using the LightCycler Probe Design software-2.0. Each sample was analysed in three independent experiments done in triplicate. Expression levels were determined with the LightCycler analysis software (version 3.5) relative to standard curves. Data were represented as the mean

level of gene expression relative to the expression of the reference gene *GAPDH*. The relative mRNA expression was calculated using the $2^{-\Delta\Delta CT}$ method.

3. Results

3.1. *ESRP1 is expressed in the undifferentiated stomach mesenchyme*

We previously developed a microarray approach to identify candidate genes involved in chicken stomach development (Le Guen et al., 2009; Notarnicola et al. 2012). Among the screened genes encoding RNA-binding proteins with high expression during the earliest stages of stomach development, we identified Epithelial Splicing Regulatory Protein 1 (*ESRP1*) (Le Guen et al., 2009). Specifically, BLAST searches in *Gallus gallus* expressed sequence tag (EST) databases allowed us to identify predicted *ESRP1* sequence that we isolated and sequenced. This sequence was deposited in the GenBank under the accession number KU679447. Using the identified *G. gallus* sequence as a query (KU679447; 607 amino acids), protein sequence alignments and phylogenetic analyses allowed us to observe high sequence similarity to human ESRP1 (80% of total homology factor, 87% of identity) confirming that the isolated sequence corresponds to the *G. gallus* ESRP1 orthologue (Fig. 1(A) and (B)).

To determine *ESRP1* expression pattern in the developing GI tract, we performed *in situ* hybridization analysis (Supplementary Fig. 1). *ESRP1* was strongly expressed in the stomach at embryonic day 4.5 (E4.5), an early stage of chicken stomach development (Fig. 1(C), left upper panel). However, its expression rapidly decreased at E7.5 (Fig. 1(C), right upper panel). *In situ* hybridization on paraffin-embedded tissue sections demonstrated that *ESRP1* transcripts were localized in the epithelial and also the mesenchymal layer of E4.5 and E6.5 stomachs (Fig. 1(C), lower panels). At E7.5, *ESRP1* expression in gastric smooth muscle is lower than at E4.5, whereas it was maintained in the gastric epithelium (Fig. 1(C), lower panels).

To confirm the unexpected *ESRP1* expression in the mesenchymal layer, we dissected and enzymatically separated the mesenchymal and epithelial layers of E4.5 stomachs (Simon-Assmann and Kedinger, 2000; Le Guen et al., 2009) and analysed *ESRP1* expression by real-time quantitative PCR (RT-qPCR). *SHH*, a specific GI epithelial marker, was used as positive control for the epithelial layer to confirm the dissection accuracy. As expected, *SHH* expression was only detected in the epithelial layer. Conversely, *ESRP1* transcripts were detected in both layers (Fig. 1(D)). Altogether, these data indicate that *ESRP1* is expressed in the epithelium and also in the undifferentiated stomach mesenchyme early during GI tract development.

3.2. *Sustained ESRP1 misexpression in the stomach mesenchyme impairs smooth muscle differentiation*

Our data indicate that *ESRP1* mesenchymal expression decreases at the onset of stomach SMC differentiation. We thus

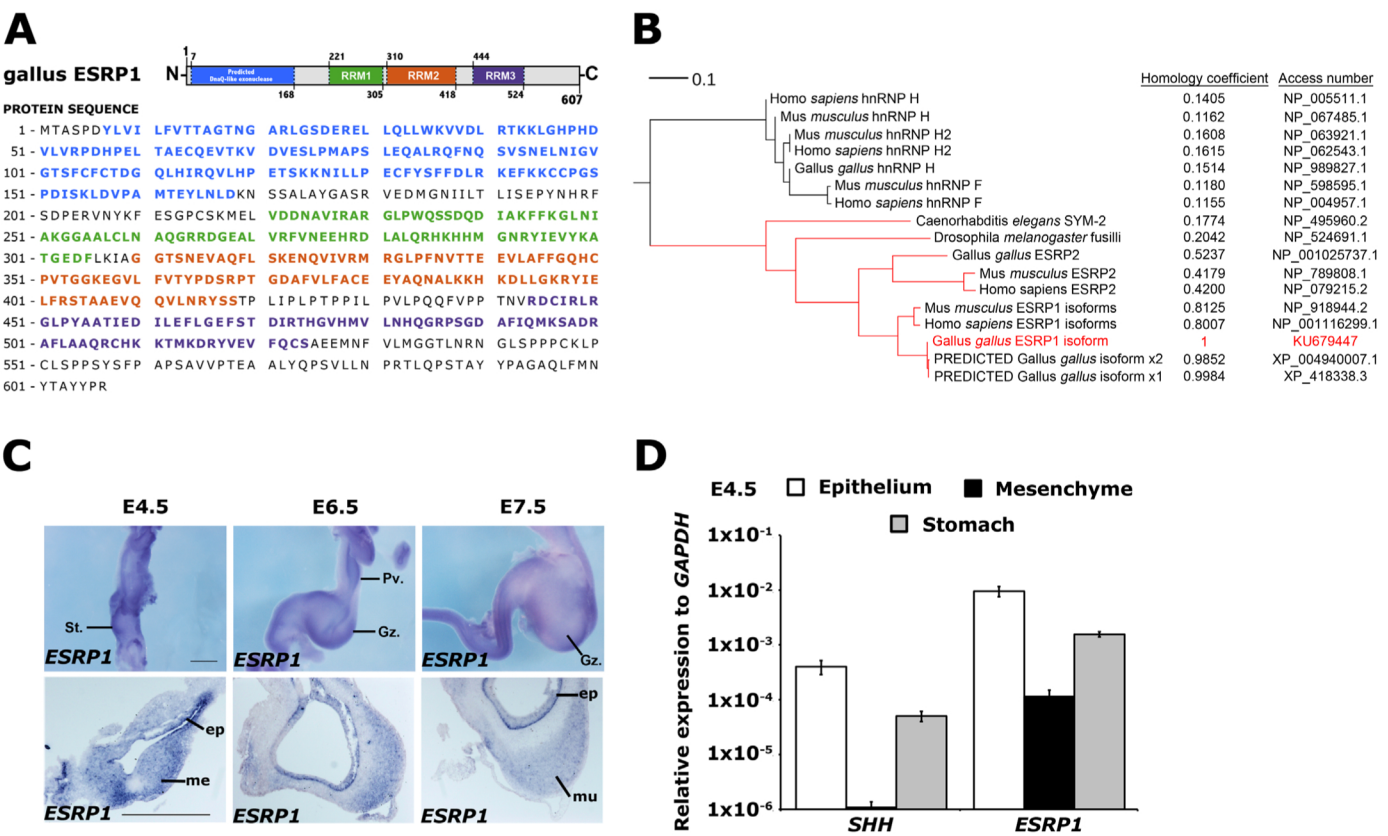

Fig. 1. ESRP1 is dynamically expressed during chick stomach mesenchyme development. (A) *Gallus gallus* ESRP1 protein sequence and domains. (B) Phylogenetic tree built using the *Gallus gallus* protein as query (in red), showing the homology coefficient compared with the query. This coefficient is a median value calculated by multiplying the coverage, identity and positivity percentages obtained after BLAST alignment of the query. The accession number of each protein is presented on the right. The scale bar represents the evolution distance of the leaf branches (in arbitrary units). Note the strong similarities of vertebrate ESRP1 orthologues with *Drosophila melanogaster* fusilli and *Caenorhabditis elegans* SYM-2. (C) *ESRP1* expression pattern during chicken stomach development. *In situ* hybridization on whole-mount (upper panels) or longitudinal stomach tissue sections (paraffin-embedded; lower panels) from E4.5, E6.5 and E7.5 chicken embryos. Scale bars: 0.5 mm. ep: epithelium; Gz: gizzard; Pv: proventriculus; me: mesenchyme; mu: muscle; St: stomach. (D) RT-qPCR analysis (mean ± standard error of the mean, in arbitrary units) of *ESRP1* and *SHH* (epithelial marker) expression in three pools of epithelium or mesenchyme layers isolated from E4.5 stomachs and in whole E4.5 stomachs (relative to *GAPDH* expression).

maintained *ESRP1* expression throughout stomach mesenchyme development and differentiation by using the avian replication-competent retroviral misexpression system (RCAS) that allows *in vivo* targeting of specific genes in the stomach mesenchyme (Moniot et al., 2004; Faure et al., 2015). Sustained *ESRP1* expression in the stomach mesenchyme did not drastically affect stomach morphogenesis compared with control (empty vector) (Fig. 2(A)). However, the gizzard (muscular stomach) area was significantly reduced in *ESRP1*-misexpressing stomachs compared to controls both at E6.5 ($1.004 \pm 0.102\ mm^2$; n=80 *versus* $1.151 \pm 0.096\ mm^2$; n=64) and E8.5 ($4.155 \pm 0.538\ mm^2$, n=22 *versus* $4.739 \pm 0.526\ mm^2$, n=18) (Fig. 2(A) and (B)). Expression of *BAPX1*, a gene involved in gizzard development and patterning (Nielsen et al., 2001; Faure et al., 2013), was not affected in *ESRP1*-misexpressing gizzards compared to controls (Supplemental Fig. 2). This suggests that the decreased gizzard size observed upon *ESRP1* misexpression was not the consequence of a change in stomach patterning. As small gizzards have already been associated with defects in SMC differentiation (Smith et al., 2000; Faure et al., 2015), we next examined by immunofluorescence the expression of determined (αSMA) and differentiated (CALPONIN and CALDESMON) SMC markers. αSMA expression was comparable in *ESRP1*-misexpressing stomachs and controls (Fig. 2(C)). Conversely, CALPONIN and CALDESMON expressions were strongly reduced in *ESRP1*-misexpressing stomachs compared to controls (Fig. 2(C), compare red with yellow arrows). These data demonstrate that sustained ESRP1 expression does not alter SMC determination. However, as stomach development proceeds, ESRP1 expression has a negative impact on further SMC differentiation.

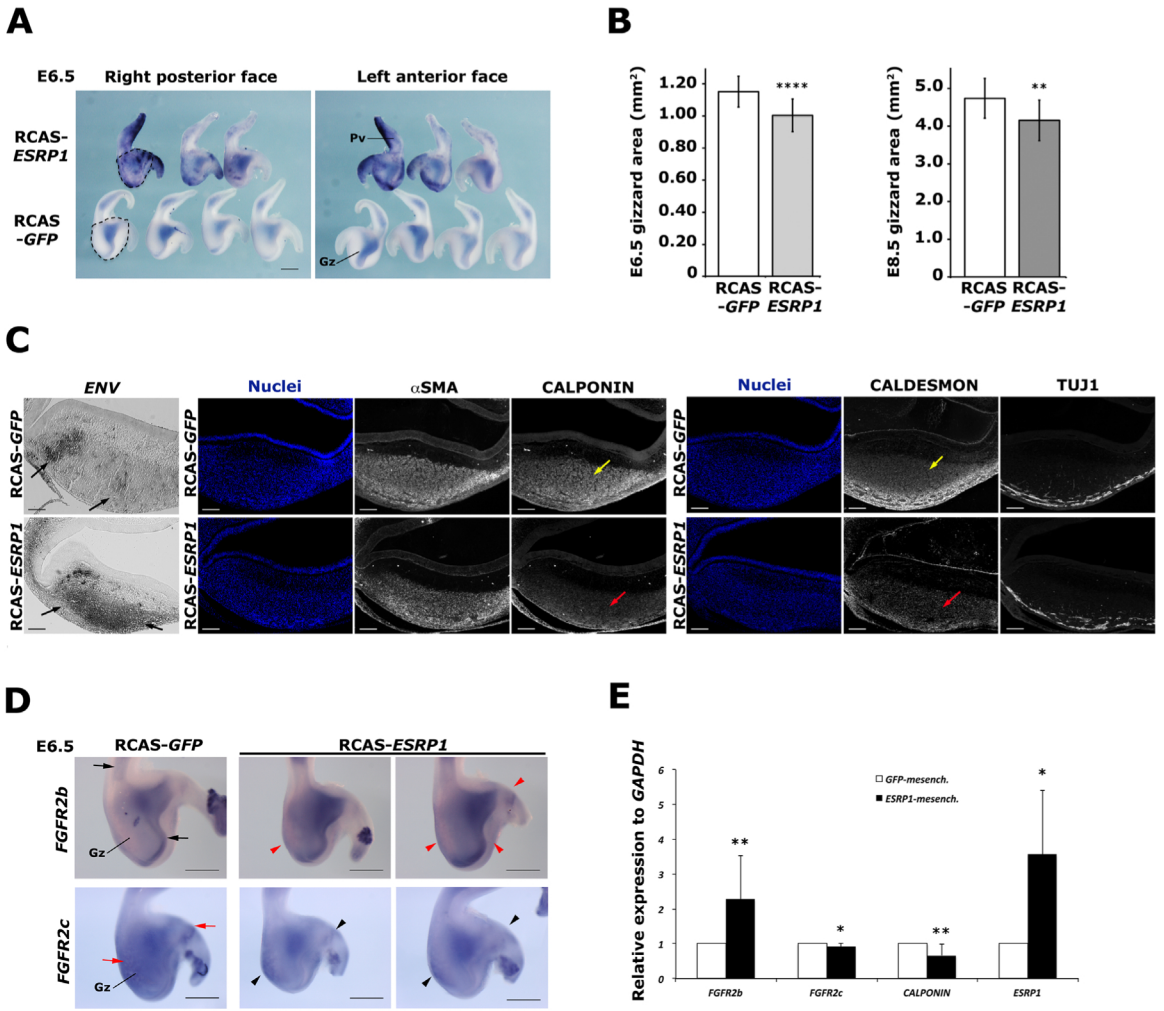

Fig. 2. Sustained *ESRP1* expression *in vivo* impairs terminal smooth muscle differentiation. (A) *ESRP1* whole-mount *in situ* hybridization on E6.5 control (RCAS-*GFP*) or *ESRP1*-misexpressing stomachs (RCAS-*ESPR1*). Note that detection of the exogenous *ESRP1* transcripts in the mesenchyme did not allow to detect the endogenous ESRP1 expression. Scale bar: 0.5 mm. Black dashed lines indicate the gizzard area for the measurement. (B) Measurement (mean ± standard error of the mean (SEM)) of the gizzard area. At E6.5 (left panel), n=64 controls *versus* n=80 *ESRP1*-misexpressing stomachs, $P < 0.0001$ by two-tailed Mann–Whitney test. At E8.5 (right panel), n=18 controls *versus* n=22 *ESRP1*-misexpressing stomachs, $P = 0.0094$). $^{**}P < 0.01$, $^{****}P < 0.0001$ by two-tailed Mann–Whitney test. (C) Serial transverse sections of control *GFP*-misexpressing (n=3) and *ESRP1*-misexpressing (n=3) E6.5 gizzards analysed either by *in situ* hybridization using the retroviral *Envelop* (*ENV*) riboprobe or by immunofluorescence with anti-αSMA, -CALPONIN -CALDESMON and –TUJ1 antibodies. Nuclei were stained with Hoechst (blue). Black arrows indicate retroviral *ENV* expression. Red arrows highlight the reduced CALPONIN and CALDESMON expression in *ESRP1*-misexpressing gizzards compared to controls (yellow arrows). Scale bar: 100 μm. (D) *In situ* hybridization analysis of *FGFR2b* (upper panels) and *FGFR2c* (lower panels) expression in control and *ESRP1*-misexpressing E6.5 stomachs. Black arrows indicate endogenous *FGFR2b* expression in the epithelium and red arrowheads the up-regulation of mesenchymal *FGFR2b* expression in *ESRP1*-misexpressing stomachs compared with control. Red arrows indicate mesenchymal *FGFR2c* expression in controls and black arrowheads the decrease of *FGFR2c* expression in *ESRP1*-misexpressing stomachs. Scale bar: 0.5 mm. Gz: gizzard. (E) RT-qPCR analysis of relative *FGFR2b*, *FGFR2c*, *CALPONIN* and *ESRP1* mRNA levels in control *GFP*- and *ESRP1*-expressing E6.5 gizzard mesenchyme. Data were normalized to *GAPDH* expression. Normalized expression levels were converted to fold changes. Values are presented as the means ± standard derivation (SD) of $n=5$ *ESRP1*-expressing *vs.* $n=5$ *GFP*-expressing gizzard mesenchyme. $^{*}P < 0.05$, $^{**}P < 0.01$, ns: not significant by one-tailed Mann-Whitney test.

ESRP1 was initially identified as a regulator of *FGFR2* splicing towards *FGFR2b* (Warzecha et al., 2009a, 2009b). Alternative splicing events between the mutually exclusive exons IIIb and IIIc of *FGFR2* (*FGFR2b* and *FGFR2c* splice variants) was previously observed during early chicken embryo development (Nishita et al., 2011). However the analysis of their levels has never been addressed during GI tract development. Therefore, we determined by whole-mount *in situ* hybridization the expression of both *FGFR2* variants in developing stomachs. At E6.5, *FGFR2b* was mainly localized in the epithelium (Fig. 2(D); black arrows in left upper panel), while *FGFR2c* was mostly detected in the mesenchyme (gizzard and pyloric structure) (Fig. 2(D); red arrows in left lower panel). Upon *ESRP1*-misexpression, mesenchymal *FGFR2b* expression increased compared to controls (Fig. 2(D), red arrowheads), whereas *FGFR2c* decreased in the mesenchyme (Fig. 2(D), black arrowheads). *FGFR2c* expression in the gizzard epithelium remained unchanged. Further analysis by RT-qPCR of dissected gizzard mesenchyme demonstrated that, compared to *GFP* control gizzard mesenchyme, *ESRP1*-misexpressing gizzard mesenchyme harboured higher levels of *FGFR2b* transcripts, whereas *FGFR2c* levels were faintly but significantly decreased (Fig. 2(E)). These findings show that sustained ESRP1 expression impairs SMC differentiation and alters *FGFR2* splicing profile in the stomach mesenchyme.

3.3. *ESRP1* overexpression induces SMC dedifferentiation

Differentiated SMCs retain the capacity to revert to less differentiated states (Owens et al., 2004; Le Guen et al., 2015; Scirocco et al., 2016) and this process can be induced by reactivation of developmental processes (Notarnicola et al., 2012; Le Guen et al., 2015). As *ESRP1* sustained expression impairs stomach SMC

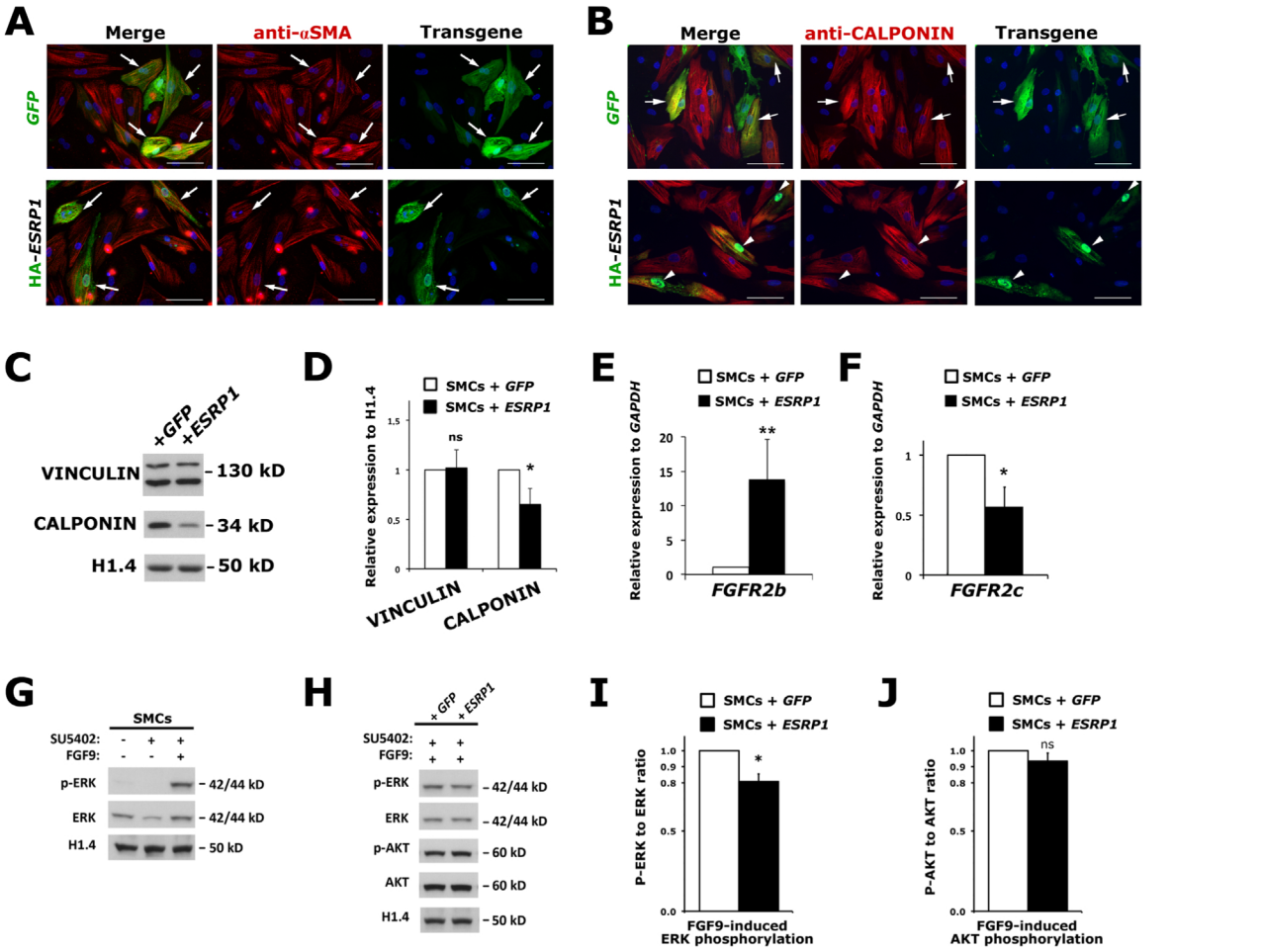

Fig. 3. ESRP1 induces SMC dedifferentiation. Primary SMCs were electroporated with *GFP* (as control) or HA-*ESRP1* constructs and after 24 h the expression of determined (αSMA) (A) and differentiated (CALPONIN) (B) SMC markers was assessed by immunofluorescence analysis. Anti-HA and -GFP antibodies were used to identify transfected cells. White arrowheads highlight the reduced CALPONIN expression in *ESRP1*-expressing cells compared with control *GFP*-expressing SMCs (white arrows). Nuclei were stained with Hoechst (blue). Scale bar: 50 μm. (C) Representative immunoblots of VINCULIN and CALPONIN expression in primary SMCs infected with RCAS-*GFP* (control) or RCAS-*ESRP1* (at day 3 after infection) for homogenous misexpression. Protein loading was verified with an anti-HISTONE H1.4 antibody. (D) Quantification of the western blots in (C). Proteins were quantified relative to HISTONE H1.4 expression. Normalized expression levels were converted to fold changes. Values are presented as the means ± SD of $n=4$ experiments. $^{*}P<0.05$, ns: non-significant by one-tailed Mann-Whitney test. (E) RT-qPCR analysis of *FGFR2c* expression in primary SMCs at day 3 after infection with RCAS-*GFP* or RCAS-*ESRP1*. Normalized expression levels were converted to fold changes. Values are presented as the means ± SD of $n=6$ experiments. $^{**}P<0.01$ by two-tailed Mann-Whitney test. (F) RT-qPCR analysis of *FGFR2c* expression in primary SMCs at day 3 after infection with RCAS-*GFP* or RCAS-*ESRP1*. Normalized expression levels were converted to fold changes. Values are presented as the means ± SD of $n=6$. $^{*}P<0.05$ by two-tailed Mann-Whitney test. (G) Representative immunoblot of phosphorylated ERK (p-ERK) and total ERK in primary SMCs pre-incubated with SU5402 (ERK phosphorylation inhibitor) before stimulation or not with recombinant FGF9. Protein loading was verified with an anti-HISTONE H1.4 antibody. (H) Representative immunoblot of phosphorylated ERK (p-ERK), ERK, phosphorylated AKT (p-AKT) and AKT in primary SMCs electroporated with *GFP*- or *ESRP1*–expressing constructs and then pre-incubated with SU5402 before stimulation with recombinant FGF9. (I and J) Quantification of the western blots in (H). ERK and AKT phosphorylation and total ERK and AKT levels were quantified relative to HISTONE H1.4 expression. The p-ERK to ERK and *p*-AKT to AKT ratios in SU5402-treated *ESRP1*-expressing SMCs. Normalized expression levels were converted to fold changes. Values are presented as the means ± SD of $n=3$. $^{*}P<0.05$, ns: non-significant by one-tailed Mann-Whitney test.

differentiation in chicken embryos (Fig. 2(C)), we next analysed the effect of ESRP1 overexpression in primary differentiated SMCs. To this aim, we isolated differentiated SMCs from E15 stomachs and cultured them on fibronectin in serum-free medium supplemented with insulin to maintain differentiation. Two days after transfection, αSMA (determination marker) and CALPONIN (differentiation marker) were homogeneously expressed in highly organized filament bundles in control SMCs (GFP-expressing vector alone) (Fig. 3(A) and (B), upper panels). In SMCs transfected with the HA-*ESRP1*-expressing construct, αSMA expression was similar to control cells (Fig. 3(A), white arrowheads in lower panels *versus* white arrows in upper panels). Conversely, CALPONIN expression was reduced compared to control SMCs (Fig. 3(B), white arrowheads in lower panels *versus* white arrows in upper panels). Western blot analysis confirmed lower CALPONIN level in *ESRP1*-expressing SMCs than in control SMCs (Fig. 3(C)). However, level of VINCULIN, an Actin-binding protein frequently used as a marker of cell-cell and cell-extracellular matrix adherens-type junctions, was not significantly affected by *ESRP1* misexpression (Ziegler et al., 2006) (Fig. 3(C) and (D)).

As *in vivo* ESRP1 controls *FGFR2* splicing (Fig. 2(D) and (E)) and forced *FgfR2b* expression inhibits SMC progenitor commitment to the SMC lineage during mouse lung development (De Langhe et al., 2006), we next analysed by RT-qPCR the transcript levels of *FGFR2* variants in cultured SMCs. ESRP1 overexpression in SMCs induced an increase in transcript levels of *FGFR2b* (Fig. 3(E)) and reduced *FGFR2c* transcript levels (Fig. 3(F)) compared to control *GFP*-expressing SMCs. Previous studies demonstrated that *FGFR2* variants have different ligand binding specificities. Specifically, the FGF9 ligand signals through FGFR2c, but not through FGFR2b (Zhang et al., 2006). Therefore, to examine FGFR2c-specific signalling activity upon FGF9 stimulation, we first incubated control SMCs with SU5420, a specific inhibitor of FGF signalling, for 2 h to abolish endogenous FGF activation. Western blot analysis confirmed that endogenous FGF activity, monitored through ERK phosphorylation ((*p*-ERK)), was inhibited upon SU5420 treatment (Fig. 3(G)). However, these SMCs could respond to FGF stimulation, as demonstrated by the increased ERK phosphorylation upon incubation with recombinant FGF9 (Fig. 3(G)). Then, we incubated both *ESRP1*- and *GFP*-expressing (control) SMCs with SU5420 before stimulation with FGF9. Quantification of western blot showed that FGF9-induced ERK phosphorylation was significantly reduced in *ESRP1*-expressing SMCs compared with control cells (Fig. 3 (H) and (I)). Conversely, AKT phosphorylation ((*p*-AKT)), which is regulated by the muscarinic pathway in SMCs (Notarnicola et al., 2012), was not affected (Fig. 3(H) and (J)). These data indicate that ESRP1 overexpression induces SMC dedifferentiation and this is associated with a change in *FGFR2* splicing and inhibition of FGFR2c-dependent ERK activity.

3.4. Synergistic effect of ESRP1 and of the RNA-binding protein RBPMS2 on SMC plasticity

Our previous (Notarnicola et al., 2012; Sagnol et al., 2014) and present findings (Fig. 3) show that the RNA-binding proteins RBPMS2 and ESRP1 are expressed in undifferentiated mesenchymal cells and that they control smooth muscle development and SMC plasticity. To assess ESRP1 and RBPMS2 role in SMC plasticity regulation, we electroporated primary differentiated SMCs with *ESRP1*- or/and *RBPMS2*- or *GFP*-expressing constructs. Immunofluorescence analysis of SMC markers one day after transfection showed that CALPONIN (differentiated SMC marker) expression was reduced, but still detectable in SMCs expressing RBPMS2 or ESRP1 alone compared to control cells (GFP alone) (Fig. 4(A)). Conversely, CALPONIN expression was completely lost in cells that co-expressed RBPMS2 and ESRP1 (Fig. 4(A), white arrowheads). Similarly, αSMA expression was faintly affected by misexpression of RBPMS2 or ESRP1 alone, but was drastically decreased when RBPMS2 and ESRP1 were co-expressed (Fig. 4(B), white arrowheads; Fig. 4(C)). These results show that ESRP1 and RBPMS2 have a synergistic effect on SMC dedifferentiation.

3.5. ESRP1 interacts with the RNA-binding protein RBPMS2

Recent reports suggest that interactions between RNA-binding proteins are important for many cellular events (Papadopoulou et al., 2010; Papadopoulou et al., 2013). We thus tested the potential interaction between ESRP1 and RBPMS2 by using coimmunoprecipitation and *in situ* Proximity Ligation Assay (PLA) approaches. Immunoprecipitation assays using an anti-Myc antibody and protein lysates from DF-1 cells that expressed Myc-tagged RBPMS2 with or without HA-tagged ESRP1 showed that HA-ESRP1 specifically co-precipitated with Myc-RBPMS2 (Fig. 5(A), lane 3). PLA experiments in DF-1 cells that co-expressed Myc-RBPMS2 and HA-ESRP1 confirmed this interaction and revealed that it occurred in the cytoplasm (Fig. 5(B)). As negative controls, we confirmed the absence of interaction of Myc-RBPMS2 or HA-ESRP1 with HA-TC10 or Myc-NICD, respectively (Supplemental Fig. S3). Finally, as RBPMS2 homodimerization through its unique RRM domain is crucial for RBPMS2-mediated regulation of SMC plasticity *in vivo*

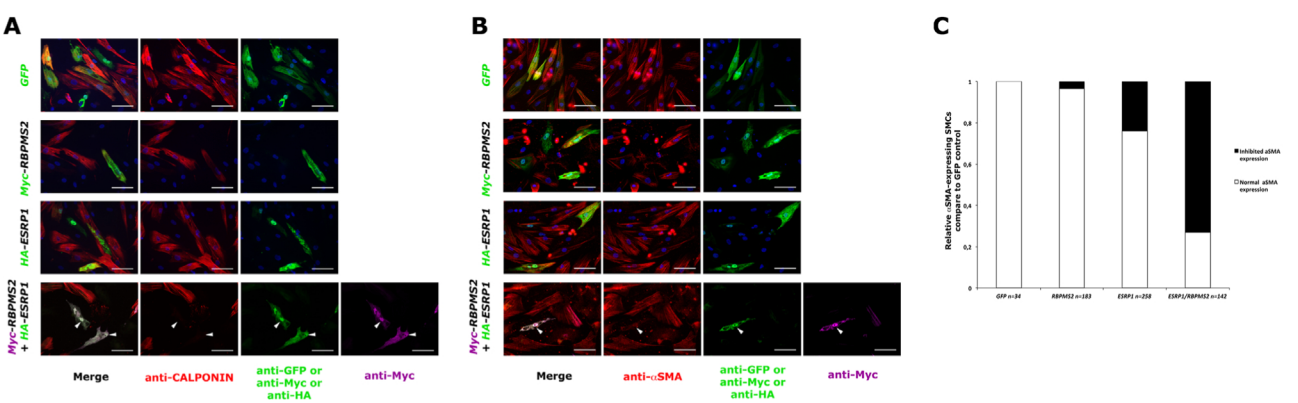

Fig. 4. ESRP1 and RBPMS2 synergistic effect on SMC dedifferentiation. Primary SMCs were electroporated with HA-*ESRP1*, Myc-*RBPMS2* or *GFP*-expressing constructs. After one day in culture, the expression of differentiated (CALPONIN) (A) and determined (αSMA) (B) SMC markers was assessed by immunofluorescence. Anti-HA, -Myc and -GFP antibodies were used to identify transfected cells. White arrowheads indicate loss of CALPONIN expression (A) or decreased αSMA expression (B) in cells that co-express ESRP1 and RBPMS2 compared with controls (*GFP*-expressing) SMCs. Nuclei were stained with Hoechst (blue). Scale bar: 50 μm. (C) Relative αSMA-expressing SMCs under *GFP*-, *ESRP1*-, *RBPMS2*- or both *ESRP1*/*RBPMS2* expressions as observed in (B). n represent the number of counted cells.

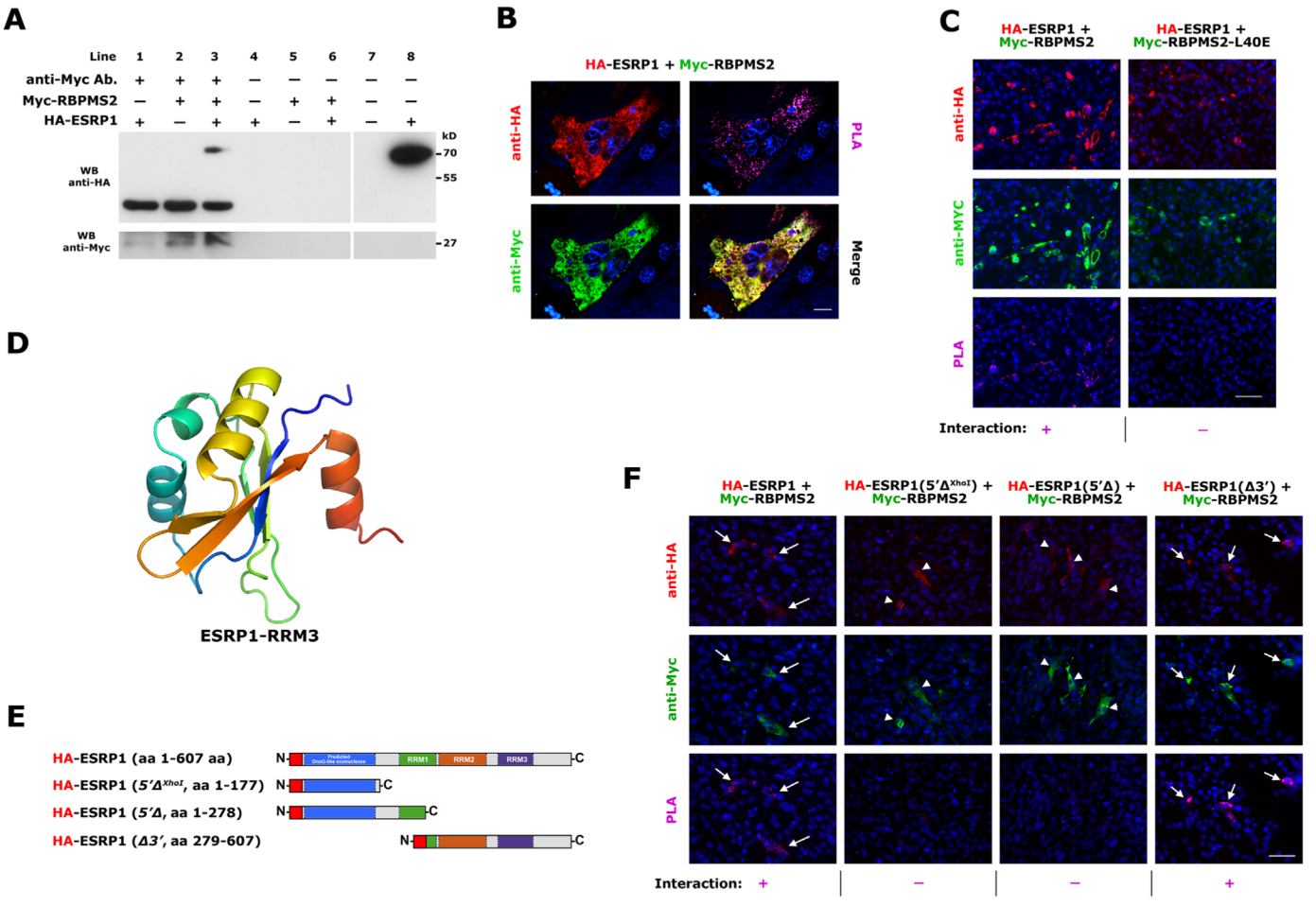

Fig. 5. ESRP1 interacts with the RNA-binding protein RBPMS2. (A) Immunoprecipitation with rabbit anti-MYC antibodies (lanes 1–3) or without (lanes 4–8) of protein lysates from DF-1 cells that express HA-ESRP1 and/or Myc-RBPMS2, as indicated. Lanes 7 and 8: 10% of total protein extracts from DF-1 cell that express HA-ESRP1 or not. Co-immunoprecipitation of HA-ESRP1 was monitored by immunoblotting with mouse anti-HA antibodies (upper panel). Note the presence of immunoglobulins in lanes 1–3. The efficiency of immunoprecipitation was monitored by immunoblotting with rabbit anti-Myc antibodies to detect Myc-RBPMS2 (lower panel). (B) Analysis of the interaction between HA-ESRP1 and Myc-RBPMS2 by Duolink Proximity Ligation Assays (PLAs) in DF-1 cells that express HA-ESRP1 and Myc-RBPMS2. HA-tagged proteins were detected with anti-mouse HA antibodies (in red) and Myc-tagged proteins with anti-rabbit Myc antibodies (in green). Protein interactions were detected with Duolink PLA labelled in magenta and were observed in the cytoplasm. Nuclei were stained with Hoechst (blue). Images were acquired by confocal microscopy. Scale bar: 10 μm. (C) Analysis of the ESPR1-RBPMS2 interaction by PLAs in DF-1 cells that co-express HA-ESRP1 and Myc-RBPMS2 or Myc-RBPMS2-L40E (a mutant that cannot dimerize). Green, anti-Myc antibody; red, anti-HA antibody; magenta, interactions between proteins detected by PLA. Nuclei were stained with Hoechst (blue). Images were acquired by epifluorescence microscopy. Scale bar: 50 μm. (D) Overall structure of human ESRP1-RRM3 solved by heteronuclear NMR experiments (ribbon diagram). The figures were prepared using Pymol (http://pymol.sourceforge.net). (E) Schematic representation of the ESRP1 constructs used in (F). (F) Analysis of the ESPR1-RBPMS2 interaction by PLA in DF-1 cells that co-express full-length or truncated HA-ESRP1, as indicated, and Myc-RBPMS2 using anti-HA (in red) and anti-Myc antibodies (in green). Interactions between proteins were detected with Duolink PLA labelled in magenta. Nuclei were stained with Hoechst (blue). White arrows indicate cells with Duolink PLA interaction, whereas white arrowheads show cells without interaction. Images were acquired by epifluorescence microscopy. Scale bar: 50 μm.

(Sagnol et al., 2014), we tested also the interaction between HA-ESRP1 and Myc-RBPMS2-L40E, a mutant in which homodimerization is inhibited. Interaction of HA-ESRP1 with the Myc-RBPMS2-L40E monomer was strongly reduced compared with wild type Myc-RBPMS2 (Fig. 5(C)). These findings indicate that ESRP1 interacts with RBPMS2 in the cytoplasm and that this interaction requires RBPMS2 homodimerization.

ESRP1 is an RNA-binding protein that contains a predicted DnaQ-like $3'-5'$ exonuclease domain in the N-terminus and three RRM domains (RRM1–3) in the C-terminal part of the protein (Fig. 1(A)). To evaluate the involvement of ESRP1 RRM domains in RBPMS2-ESRP1 interaction we first structurally characterized RRM3. By using NMR spectroscopy and $^{15}N/^{13}C$-labelled recombinant human ESRP1-RRM3 (residues 439–539), we assigned more than 98% of the amide group resonances to the non-proline residues (4 prolines over 104 residues) and solved the high-resolution NMR structure of ESRP1-RRM3 (Fig. 5(D), Supplemental Table 1 and Supplemental Fig. 4A). Human ESRP1-RRM3 shares a similar 3D fold with other RRM domains. This fold consists of a twisted antiparallel β-sheet formed by four β-strands (β1: C^{446}-R^{450}; β2: V^{477}-V^{480}; β3: D^{490}-Q^{494}; β4: E^{519}-C^{523}), two α-helices (α1: I^{458}-L^{465}, E^{467}-D^{471}; α2: A^{498}-C^{508}) on one side of the β-sheet and one C-terminal α-helix (α3: A^{525}-M^{533}) on the other side (Fig. 5(D)). Identical NMR spectra were obtained for $^{15}N/^{13}C$-labelled ESPR1-RRM3 in the absence or presence of unlabelled RBPMS2-RRM. This indicates that the ESRP1 RRM3 domain does not interact with the RRM domain of RBPMS2 (Supplemental Fig. 4B). Therefore, to identify the ESRP1 sequence required for the interaction with RBPMS2, we performed *in situ* PLA in DF-1 cells that co-expressed Myc-RBPMS2 and different ESRP1 truncated variants tagged with HA (Fig. 5(E)). Interaction with RBPMS2 occurred only in cells that co-expressed the C-terminal part of ESPR1, which included the RRM2 and RRM3 domains, but not in cells that co-expressed ESRP1 N-terminal region (Fig. 5(F), compare white arrows with white arrowheads).

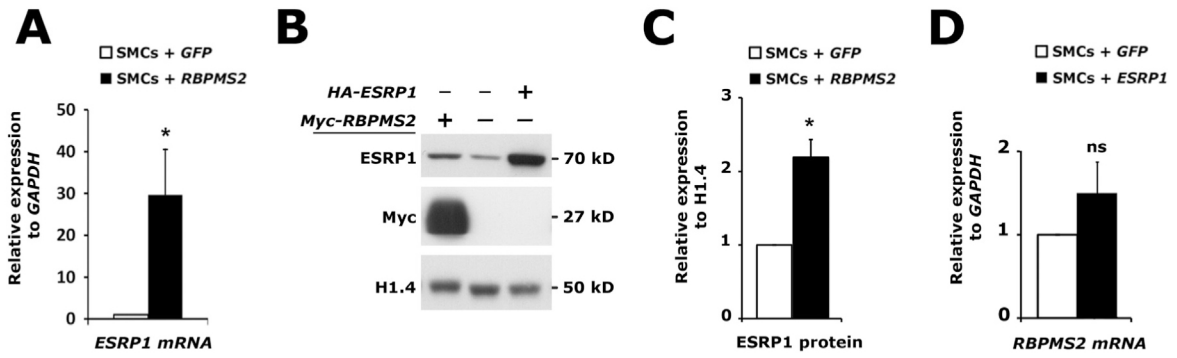

Fig. 6. Regulation of ESRP1 expression by RBPMS2. (A) RT-qPCR analysis (three independent experiments) of *ESRP1* expression in primary SMCs infected with RCAS-*GFP* or RCAS-Myc-*RBPMS2* (day 3 post-infection). Normalized expression levels were converted to fold changes. Values are presented as the means ± SD of n = 3 experiments. $^{*}P < 0.05$ by two-tailed Mann-Whitney test. (B) Representative immunoblot of ESRP1 expression in primary SMCs electroporated with the pCSH-*ESRP1* or RCAS-Myc-*RBPMS2* constructs. Protein loading was verified with an anti-HISTONE H1.4 antibody. (C) Quantification of the western blots in (B). ESRP1 levels were quantified relative to HISTONE H1.4 expression. Normalized expression levels were converted to fold changes. Values are presented as the means ± SD of n = 3. $^{*}P < 0.05$ by one-tailed Mann-Whitney test.. (D) RT-qPCR analysis (three independent experiments) of *RBPMS2* expression in primary SMCs infected with RCAS-*GFP* or RCAS-*ESRP1* (day 3 post-infection). Normalized expression levels were converted to fold changes. Values are presented as the means ± SD of n = 3 experiments. ns: not significant by two-tailed Mann-Whitney test.

3.6. *RBPMS2-dependent regulation of SMC plasticity requires ESRP1*

As ESRP1 and RBPMS2 both induce dedifferentiation of SMCs in culture, we asked whether they mutually regulated their expression during this process. RT-qPCR and western blot analyses revealed that RBPMS2 overexpression in cultured primary SMCs significantly induces an upregulation of *ESRP1* transcript (Fig. 6(A)) and protein levels (Fig. 6(B) and (C)) compared to control SMCs (*GFP* expression only). Conversely, ESRP1 overexpression did not significantly affect *RBPMS2* expression level (Fig. 6(D)).

Then, to examine ESPR1 role in RBPMS2-mediated regulation of SMC plasticity, we silenced *ESRP1* in primary SMCs. Compared to control (GFP-shSCRAMBLE), expression in cultured SMCs of a GFP-labelled shRNA against *ESRP1* (GFP-sh*ESRP1*) decreased both ESRP1 mRNA and protein level without affecting CALPONIN expression (Fig. 7(A)–(C)). After cell sorting by FACS based on GFP expression, we assessed CALPONIN expression in differentiated SMCs transfected with Myc-*RBPMS2*- and GFP-sh*ESRP1*- or GFP-shSCRAMBLE-expressing constructs (Fig. 7(D)). Immunofluorescence analysis indicated that CALPONIN expression was completely lost in SMCs that co-expressed RBPMS2 and shSCRAMBLE (Fig. 7(D), white arrows). Conversely, CALPONIN expression was not affected in SMCs co-expressing *RBPMS2* and sh*ESRP1* (Fig. 7(D); white arrowheads). Western blotting analyses confirmed that *RBPMS2* misexpression induced an increased in ESRP1 protein level and this was associated with a decrease in CALPONIN protein level (Fig. 7(E)). However, when the upregulation of ESRP1 upon *RBPMS2* misexpression was partially silenced in SMCs with sh*ESRP1* construct, CALPONIN protein expression was also partially rescued (Fig. 7(E) and (F), compare *RBPMS2*/sh*ESRP1* to both *RBPMS2*/shSCRAMBLE and HA-empty/shSCRAMBLE conditions). Altogether, these findings demonstrate that ESRP1 is essential for RBPMS2-dependent SMC dedifferentiation.

4. Discussion

In this study, we found that *ESRP1* is expressed also during the early phase of gastrointestinal mesenchyme development. Moreover, *ESRP1* sustained expression in gastrointestinal SMCs promotes the switch from *FGFR2c* to *FGFR2b* splicing and inhibits CALPONIN expression (a marker of differentiated SMC) both *in vivo* and in primary SMCs. ESRP1 is a tumour suppressor gene that is mutated in 50% of primary colon tumours with microsatellite instability (Ivanov et al., 2007; Leontieva et al., 2009). ESRP1 promotes the alternative splicing of transcripts that switch splicing during mesenchymal to epithelial transition (Warzecha et al., 2009a, 2009b, 2010). Although ESRP1 has been mainly studied during cancer-related processes (Warzecha and Carstens, 2012), its expression is altered also in cardiac hypertrophy (Kim et al., 2014). Moreover, ESRP1 is expressed and functional during *Xenopus laevis* epidermis development (Castello et al., 2013). This and our results suggest that ESRP1 expression and function could be related to the regulation/maintenance of the immature status of gastrointestinal SMCs. In agreement, ESRP1 was listed in the RNA-binding protein repertoire of embryonic stem cells (Kwon et al., 2013) and regulates the expression of pluripotency-related factors in mouse embryonic stem cells (Fagoonee et al., 2013). Altogether, these data support the hypothesis that besides its role in epithelial homeostasis and mesenchymal to epithelial transition, ESRP1 could have a broader role in immature cells.

We previously identified the RNA-binding protein RBPMS2 as an early marker of gastrointestinal mesenchyme and a critical activator of gastrointestinal SMC dedifferentiation (Notarnicola et al., 2012). RBPMS2 stimulates the expression of and binds to *NOGGIN* mRNA, leading to inhibition of the BMP signalling pathway in chicken embryos (Notarnicola et al., 2012; Sagnol et al., 2014). The morphogen NOGGIN promotes SMC dedifferentiation, but cannot stimulate SMC proliferation, differently from RBPMS2. In addition, in chick embryos, ectopic expression of RBPMS2 in few SMCs induces the expression of NOGGIN that can diffuse to all SMCs and contributes to inhibiting their differentiation. However, treatment with BMP4 restores differentiation only in SMCs that do not misexpress RBPMS2, suggesting that in addition to the BMP pathway, RBPMS2 regulates also other pathways involved in SMC plasticity (Notarnicola et al., 2012). Here, we found that RBPMS2 interacts with ESRP1. Like RBPMS2, ESRP1 is expressed transiently in the undifferentiated gastrointestinal mesenchyme during the early stages of GI development. Moreover, RBPMS2 misexpression in SMCs induces ESRP1 mRNA and protein expression and when co-expressed, ESRP1 and RBPMS2 show synergistic effects on SMC dedifferentiation. Finally, by down-regulating *ESRP1* expression, we demonstrate that RBPMS2 requires ESRP1 to induce SMC dedifferentiation, strengthening the importance of this interaction. As RBPMS2 and ESRP1 regulate different pathways (the BMP and FGF signalling cascades, respectively), we hypothesize that the precise regulation of these pathways is required to control the switch between differentiated and proliferative SMCs (Fig. 8). Our study mainly focused on the expression and function of ESRP1 during the development of stomach smooth muscle. However, we can hypothesize that ESRP1 could act on similar way in other gut region. To support this, we previously demonstrated that *RBPMS2*

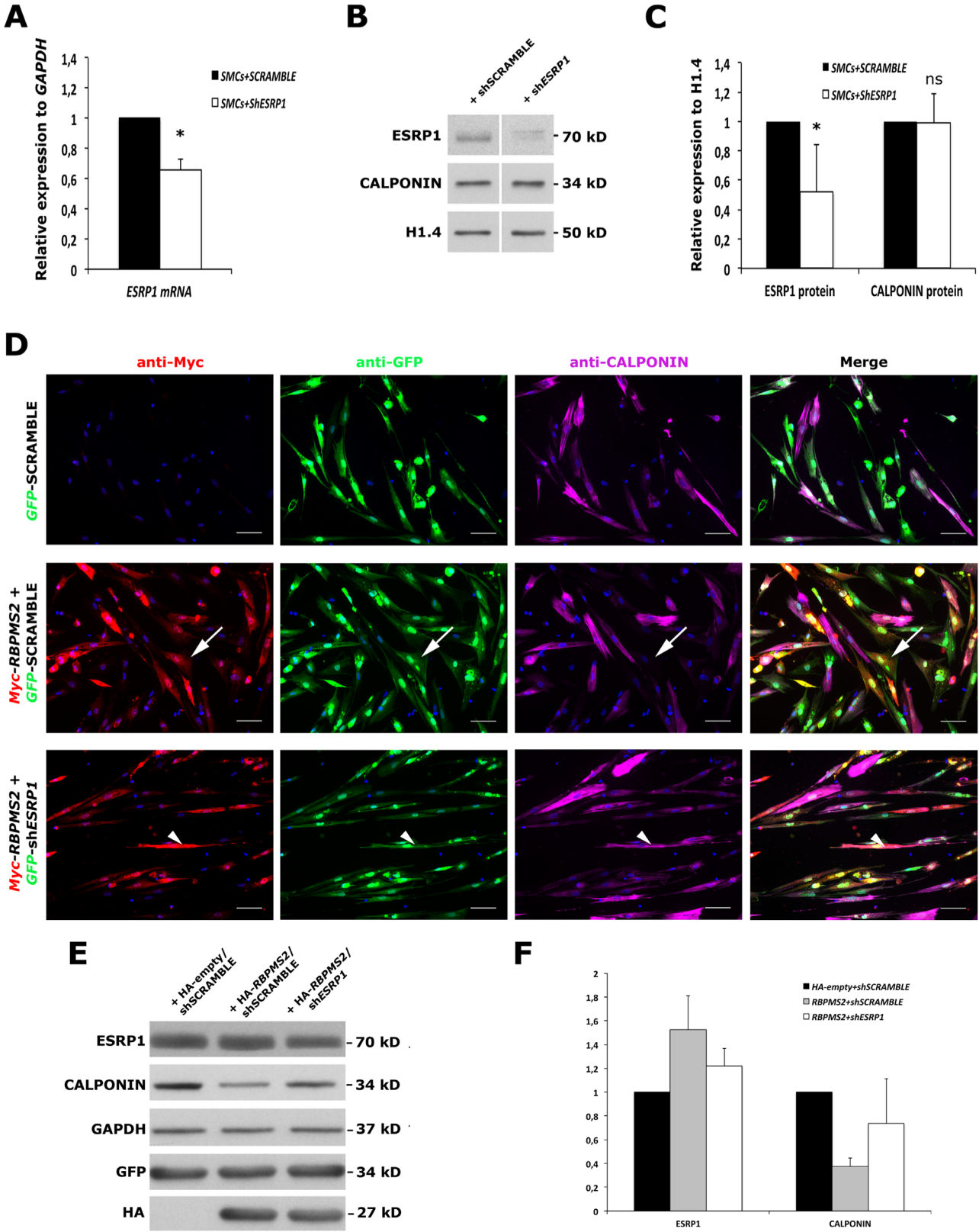
A
Relative expression to GAPDH
1,4
1,2
1
0,8
0,6
0,4
0,2
0
SMCs+SCRAMBLE
SMCs+ShESRP1
*
ESRP1 mRNA
B
+ shSCRAMBLE
+ shESRP1
ESRP1
CALPONIN
H1.4
70 kD
34 kD
50 kD
C
Relative expression to H1.4
SMCs+SCRAMBLE
SMCs+ShESRP1
*
ns
ESRP1 protein
CALPONIN protein
D
anti-Myc
anti-GFP
anti-CALPONIN
Merge
GFP-SCRAMBLE
Myc-RBPMS2 +
GFP-SCRAMBLE
Myc-RBPMS2 +
GFP-shESRP1
E
+ HA-empty/
shSCRAMBLE
+ HA-RBPMS2/
shSCRAMBLE
+ HA-RBPMS2/
shESRP1
ESRP1
CALPONIN
GAPDH
GFP
HA
70 kD
34 kD
37 kD
34 kD
27 kD
F
2
1,8
1,6
1,4
1,2
1
0,8
0,6
0,4
0,2
0
HA-empty+shSCRAMBLE
RBPMS2+shSCRAMBLE
RBPMS2+shESRP1
ESRP1
CALPONIN

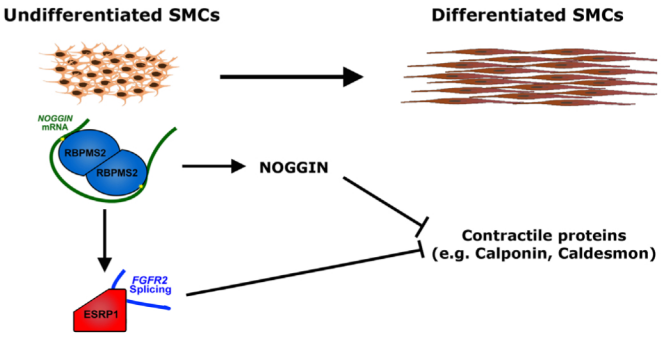

Fig. 8. Model of the gastrointestinal SMC development regulated by ESRP1, RBPMS2 and their downstream signalling pathways FGFR2 and BMP.

misexpression impairs smooth muscle differentiation in the stomach, but also in colon musculature *in vivo* (Notarnicola et al., 2012). Further investigations are required to examine how ESRP1/RBPMS2 and BMP/FGF signalling cascades could be regulators of smooth muscle development in other gut regions.

Vertebrate RBPMS2 forms stable homodimers *in vitro* and *in vivo via* the RRM domain and its homodimerization is functionally required to drive RBPMS2-dependent SMC dedifferentiation through up-regulation of *NOGGIN* mRNA (Sagnol et al., 2014). Here, we found that ESRP1 interacts with RBPMS2, but not with a mutant that cannot form homodimers. The specific motif in the RRM domain required for RBPMS2 homodimerization is conserved in the orthologue proteins Couch Potato (CPO) in *Drosophila melanogaster* and MEC-8 in *Caenorhabditis elegans* (Sagnol et al., 2014). Based on sequence similarities, we found that *D. melanogaster* fusilli and *C. elegans* SYM-2 are ESRP1 orthologues (Fig. 1 (B)). Genetic analyses during embryonic development indicate that *sym-2* has redundant functions with *mec-8* in regulating the structure of body wall muscles and their attachment to the body cuticle (Davies et al., 1999; Yochem et al., 2004). Altogether, these findings highlight the functional conservation of ESRP1-RBPMS2 interaction, possibly in regulating the maturation of transcripts essential for embryonic development and SMC plasticity.

Acknowledgments

This work was funded by grants from the Association Française contre les Myopathies (AFM) (Nos. 16413 and 18766), the French Infrastructure for Integrated Structural Biology (FRISBI) and the French Patients' Association POIC to P.d.S.B.; S.S. had a University Montpellier 1 post-doctoral fellowship. We thank Sandrine Faure for important intellectual contributions during this work and critical revision of the manuscript.

References

Bebee, T.W., Park, J.W., Sheridan, K.I., Warzecha, C.C., Cieply, B.W., Rohacek, A.M., Xing, Y., Carstens, R.P., 2015. The splicing regulators Esrp1 and Esrp2 direct an epithelial splicing program essential for mammalian development. Elife 4, e08954.

Brown, R.L., Reinke, L.M., Damerow, M.S., Perez, D., Chodosh, L.A., Yang, J., Cheng, C., 2011. CD44 splice isoform switching in human and mouse epithelium is essential for epithelial-mesenchymal transition and breast cancer progression. J. Clin. Investig. 121, 1064–1074.

Castello, A., Fischer, B., Hentze, M.W., Preiss, T., 2013. RNA-binding proteins in Mendelian disease. Trends Genet. 29, 318–327.

Davies, A.G., Spike, C.A., Shaw, J.E., Herman, R.K., 1999. Functional overlap between the mec-8 gene and five sym genes in *Caenorhabditis elegans*. Genetics 153, 117–134.

De Langhe, S.P., Carraro, G., Warburton, D., Hajihosseini, M.K., Bellusci, S., 2006. Levels of mesenchymal FGFR2 signaling modulate smooth muscle progenitor cell commitment in the lung. Dev. Biol. 299, 52–62.

de Santa Barbara, P., van den Brink, G.R., Roberts, D.J., 2002. Molecular etiology of gut malformations and diseases. Am. J. Med. Genet. 115, 221–230.

De Santa Barbara, P., Williams, J., Goldstein, A.M., Doyle, A.M., Nielsen, C., Winfield, S., Faure, S., Roberts, D.J., 2005. Bone morphogenetic protein signaling pathway plays multiple roles during gastrointestinal tract development. Dev. Dyn. 234, 312–322.

Fagoonee, S., Bearzi, C., Di Cunto, F., Clohessy, J.G., Rizzi, R., Reschke, M., Tolosano, E., Provero, P., Pandolfi, P.P., Silengo, L., Altruda, F., 2013. The RNA binding protein ESRP1 fine-tunes the expression of pluripotency-related factors in mouse embryonic stem cells. PLoS One 8, e72300.

Faure, S., de Santa Barbara, P., 2011. Molecular embryology of the foregut. J. Pediatr. Gastroenterol. Nutr. 52, S2–S3.

Faure, S., Georges, M., McKey, J., Sagnol, S., de Santa Barbara, P., 2013. Expression pattern of the homeotic gene Bapx1 during early chick gastrointestinal tract development. Gene Expr. Patterns 13, 287–292.

Faure, S., McKey, J., Sagnol, S., de Santa Barbara, P., 2015. Enteric neural crest cells regulate vertebrate stomach patterning and differentiation. Development 142, 331–342.

Gabella, G., 2002. Development of visceral smooth muscle. Results Probl. Cell Differ. 38, 1–37.

Gerstberger, S., Hafner, M., Ascano, M., Tuschl, T., 2014. Evolutionary conservation and expression of human RNA-binding proteins and their role in human genetic disease. Adv. Exp. Med. Biol. 825, 1–55.

Hnia, K., Notarnicola, C., de Santa Barbara, P., Hugon, G., Rivier, F., Laoudj-Chenivesse, D., Mornet, D., 2008. Biochemical properties of gastrokine-1 purified from chicken gizzard smooth muscle. PLoS One 3, e3854.

Ivanov, I., Lo, K.C., Hawthorn, L., Cowell, J.K., Ionov, Y., 2007. Identifying candidate colon cancer tumor suppressor genes using inhibition of nonsense-mediated mRNA decay in colon cancer cells. Oncogene 26, 2873–2884.

Kim, T., Kim, J.O., Oh, J.G., Hong, S.E., Kim do, H., 2014. Pressure-overload cardiac hypertrophy is associated with distinct alternative splicing due to altered expression of splicing factors. Mol. Cells 37, 81–87.

Kwon, S.C., Yi, H., Eichelbaum, K., Fohr, S., Fischer, B., You, K.T., Castello, A., Krijgsveld, J., Hentze, M.W., Kim, V.N., 2013. The RNA-binding protein repertoire of embryonic stem cells. Nat. Struct. Mol. Biol. 20, 1122–1130.

Le Guen, L., Marchal, S., Faure, S., de Santa Barbara, P., 2015. Mesenchymal-epithelial interactions during digestive tract development and epithelial stem cell regeneration. Cell. Mol. Life Sci. 72, 3883–3896.

Le Guen, L., Notarnicola, C., de Santa Barbara, P., 2009. Intermuscular tendons are essential for the development of vertebrate stomach. Development 136, 791–801.

Leontieva, O.V., Ionov, Y., 2009. RNA-binding motif protein 35A is a novel tumor suppressor for colorectal cancer. Cell Cycle 8, 490–497.

Fig. 7. ESRP1 is required for RBPMS2-dependent regulation of SMC plasticity. (A) Relative quantification by RT-qPCR for *ESRP1* mRNA expression in ShSCRAMBLE- or Sh*ESRP1*-expressing SMCs FACS-sorted for GFP expression. Normalized expression levels were converted to fold changes. Values are presented as the means ± SD of n = 3 experiments. $^{*}P < 0.05$ by one-tailed Mann-Whitney test. (B) Representative western blot analysis of ESRP1, CALPONIN and HISTONE H1.4 expression in ShSCRAMBLE- and Sh*ESRP1*-expressing SMCs FACS-sorted for GFP expression. (C) Quantification relative to HISTONE H1.4 expression of the western blots in (B). Normalized expression levels were converted to fold changes. Values are presented as the means ± SD of n = 3 experiments. $^{*}P < 0.05$, ns: not significant by one-tailed Mann-Whitney test. (D) Immunofluorescence analysis of primary SMCs electroporated with Myc-*RBPMS2*, GFP-ShSCRAMBLE or GFP-Sh*ESRP1* constructs, as indicated. In each condition, SMCs were electroporated with the same amount of GFP-expressing plasmid and the day after SMCs were sorted by FACS based on GFP expression, before analysis with anti-CALPONIN (differentiated SMC marker), -Myc and –GFP antibodies. White arrows indicate loss of CALPONIN expression in cells that co-express RBPMS2 and ShSCRAMBLE. White arrowheads indicate maintenance of CALPONIN expression in cells that co-express *RBPMS2* and sh*ESRP1*. Nuclei were stained with Hoechst (blue). Scale bar: 50 μm. (E) Representative immunoblot of CALPONIN expression in primary SMCs electroporated with the HA-*RBPMS2* and ShSCRAMBLE or Sh*ESRP1* constructs compare to control SMCs electroporated with the HA-empty and shSCRAMBLE constructs. In each condition, SMCs were electroporated with the same amount of *GFP*-expressing plasmid and the day after, GFP-positive SMCs were sorted by FACS. Protein loading was verified by GAPDH expression. (F) Quantification relative to GAPDH expression of the western blots in (E). Normalized expression levels were converted to fold changes compare to HA-empty/shSCRAMBLE condition. Values are presented as the means ± SD of n = 2 experiments.

Moniot, B., Biau, S., Faure, S., Nielsen, C.M., Berta, P., Roberts, D.J., de Santa Barbara, P., 2004. SOX9 specifies the pyloric sphincter epithelium through mesenchymal-epithelial signals. Development 131, 3795–3804.
Nielsen, C., Murtaugh, L.C., Chyung, J.C., Lassar, A., Roberts, D.J., 2001. Gizzard formation and the role of Bapx1. Dev. Biol. 231, 164–174.
Nishita, J., Ohta, S., Bleyl, S.B., Schoenwolf, G.C., 2011. Detection of isoform-specific fibroblast growth factor receptors by whole-mount *in situ* hybridization in early chick embryos. Dev. Dyn. 240, 1537–1547.
Notarnicola, C., Rouleau, C., Le Guen, L., Virsolvy, A., Richard, S., Faure, S., De Santa Barbara, P., 2012. The RNA-binding protein RBPMS2 regulates development of gastrointestinal smooth muscle. Gastroenterology 143 (687–697), e681–e689.
Owens, G.K., Kumar, M.S., Wamhoff, B.R., 2004. Molecular regulation of vascular smooth muscle cell differentiation in development and disease. Physiol. Rev. 84, 767–801.
Papadopoulou, C., Patrinou-Georgoula, M., Guialis, A., 2010. Extensive association of HuR with hnRNP proteins within immunoselected hnRNP and mRNP complexes. Biochim. Biophys. Acta 1804, 692–703.
Papadopoulou, C., Ganou, V., Patrinou-Georgoula, M., Guialis, A., 2013. HuR-hnRNP interactions and the effect of cellular stress. Mol. Cell. Biochem. 372, 137–147.
Revil, T., Jerome-Majewska, L.A., 2013. During embryogenesis, esrp1 expression is restricted to a subset of epithelial cells and is associated with splicing of a number of developmentally important genes. Dev. Dyn. 242, 281–290.
Sagnol, S., Yang, Y., Bessin, Y., Allemand, F., Hapkova, I., Notarnicola, C., Guichou, J.F., Faure, S., Labesse, G., de Santa Barbara, P., 2014. Homodimerization of RBPMS2 through a new RRM-interaction motif is necessary to control smooth muscle plasticity. Nucleic Acids Res. 42, 10173–10184.
Scirocco, A., Matarrese, P., Carabotti, M., Ascione, B., Malorni, W., Severi, C., 2016. Cellular and molecular mechanisms of phenotypic switch in gastrointestinal smooth muscle. J. Cell. Physiol. 231, 295–302.
Simon-Assmann, P., Kedinger, M., 2000. Tissue recombinants to study extracellular matrix targeting to basement membranes. Methods Mol. Biol. 139, 311–319.
Smith, D.M., Nielsen, C., Tabin, C.J., Roberts, D.J., 2000. Roles of BMP signaling and Nkx2.5 in patterning at the chick midgut-foregut boundary. Development 127, 3671–3681.
Soderberg, O., Leuchowius, K.J., Gullberg, M., Jarvius, M., Weibrecht, I., Larsson, L.G., Landegren, U., 2008. Characterizing proteins and their interactions in cells and tissues using the *in situ* proximity ligation assay. Methods 45, 227–232.
Warzecha, C.C., Carstens, R.P., 2012. Complex changes in alternative pre-mRNA splicing play a central role in the epithelial-to-mesenchymal transition (EMT). Semin. Cancer Biol. 22, 417–427.
Warzecha, C.C., Jiang, P., Amirikian, K., Dittmar, K.A., Lu, H., Shen, S., Guo, W., Xing, Y., Carstens, R.P., 2010. An ESRP-regulated splicing programme is abrogated during the epithelial-mesenchymal transition. EMBO J. 29, 3286–3300.
Warzecha, C.C., Sato, T.K., Nabet, B., Hogenesch, J.B., Carstens, R.P., 2009a. ESRP1 and ESRP2 are epithelial cell-type-specific regulators of FGFR2 splicing. Mol. Cell 33, 591–601.
Warzecha, C.C., Shen, S., Xing, Y., Carstens, R.P., 2009b. The epithelial splicing factors ESRP1 and ESRP2 positively and negatively regulate diverse types of alternative splicing events. RNA Biol. 6, 546–562.
Yae, T., Tsuchihashi, K., Ishimoto, T., Motohara, T., Yoshikawa, M., Yoshida, G.J., Wada, T., Masuko, T., Mogushi, K., Tanaka, H., Osawa, T., Kanki, Y., Minami, T., Aburatani, H., Ohmura, M., Kubo, A., Suematsu, M., Takahashi, K., Saya, H., Nagano, O., 2012. Alternative splicing of CD44 mRNA by ESRP1 enhances lung colonization of metastatic cancer cell. Nat. Commun. 3 (883), e1892.
Yochem, J., Bell, L.R., Herman, R.K., 2004. The identities of sym-2, sym-3 and sym-4, three genes that are synthetically lethal with mec-8 in *Caenorhabditis elegans*. Genetics 168, 1293–1306.
Zhang, X., Ibrahimi, O.A., Olsen, S.K., Umemori, H., Mohammadi, M., Ornitz, D.M., 2006. Receptor specificity of the fibroblast growth factor family. The complete mammalian FGF family. J. Biol. Chem. 281, 15694–15700.
Ziegler, W.H., Liddington, R.C., Critchley, D.R., 2006. The structure and regulation of vinculin. Trends Cell Biol. 16, 453–460.